

GEOMETRIC MODELING OF THE UNFOLDING OF A ROD STRUCTURE IN THE FORM OF A DOUBLE SPHERICAL PENDULUM IN WEIGHTLESSNESS

L. Kutsenko

Doctor of Technical Sciences, Professor
Department of Engineering and Rescue Technology*
E-mail: leokuts@i.ua

O. Semkiv

Doctor of Technical Sciences, Vice-Rector
Department of prevention activities and monitoring*

V. Asotskyi

PhD Scientific and methodical center of
educational institutions in the field of civil protection*

L. Zapolskiy

PhD, Senior Researcher
Department of Scientific and organizational
Ukrainian Civil Protection Research Institute
Rybalska str., 18, Kyiv, Ukraine, 01011

O. Shoman

Doctor of Technical Sciences, Professor, Head of Department**

N. Ismailova

Doctor of Technical Sciences, Associate Professor
Department of Engineering Mechanics
Military Academy
Fontanska doroha str., 10, Odessa, Ukraine, 65009

V. Danylenko

Associate Professor
Department of Engineering and Computer Graphics
Kharkiv National Automobile and Highway University
Yaroslava Mudroho str., 25, Kharkiv, Ukraine, 61002

S. Vinogradov

PhD, Associate Professor
Department of Engineering and Rescue Technology*

E. Sivak

PhD, Associate Professor **
*National University of Civil Defense of Ukraine
Chernyshevska str., 94, Kharkiv, Ukraine, 61023

**Department of Geometrical Modeling and Computer Graphics
National Technical University "Kharkiv Polytechnic Institute"
Kyrpychova str., 2, Kharkiv, Ukraine, 61002

Досліджено геометричну модель нового способу розкриття в умовах невагомості стержневої конструкції, подібної подвійному сферичному маятнику. Переміщення елементів конструкції відбуваються завдяки дії імпульсів піротехнічних реактивних двигунів на кінцеві точки ланок. Опис руху одержаного інерційного розкриття стержневої конструкції виконано за допомогою рівняння Лагранжа другого роду, і, зважаючи на умови невагомості, побудовано з використанням лише кінетичної енергії системи.

На актуальність обраної теми вказує необхідність вибору та дослідження процесу активізації розкриття просторової стержневої конструкції. В якості рушіїв пропонується використати імпульсні піротехнічні реактивні двигуни, встановлені на кінцевих точках ланок конструкції. Легші і дешевші порівняно, наприклад, з електродвигунами або пружинними пристроями. А також економічно вигідніші, коли процес розкриття конструкції на орбіті планується виконати лише один раз.

Запропоновано спосіб визначення параметрів та початкових умов ініціювання коливань подвійної стержневої конструкції з метою одержання циклічної траєкторії кінцевої точки другої ланки. Це дозволяє при розрахунках процесу трансформування уникати хаотичних рухів елементів конструкції. Побудовано графіки зміни у часі функцій узагальнених координат, а також перших та других похідних цих функцій. Тому з'явилася можливість оцінити силові характеристики системи в момент гальмування (стопоріння) процесу розкриття.

Результати можуть використовуватися як геометричні моделі варіантів розкриття великогабаритних об'єктів в умовах невагомості, наприклад, силових каркасів космічних антен чи фермених конструкцій, а також інших орбітальних інфраструктур

Ключові слова: стержнева конструкція, процес розкриття у космосі, двохланкова сферична конструкція, рівняння Лагранжа другого роду

1. Introduction

The construction of frames for orbital space infrastructures is associated with the transformation of rod structures in order to provide their required spatial position. Components

of structures are delivered into orbit in a folded form. Thus, a certain technology for transforming location the rods is needed so that the entire structure acquires the planned spatial shape. Such transformations are performed using the mechanical operation of unfolding [1, 2]. When transport-

ing from the Earth, the structure workpieces take the form mostly of rectilinear rods that are connected similar to the elements of a multi-link pendulum. The unfolding of a double rod structure is expedient to consider as an equivalent of the "oscillation" of a double spherical pendulum in weightlessness. Controlling the unfolding of large structures in space is a complex scientific and technical task of mechanics as it has no analogues in the ground-based technology. It is relatively easy to implement it for a double (two-link) rod structure. We shall note that the term "pendulum" is not readily applicable in the case of weightlessness. Therefore, hereafter we shall use mostly the term "a double spherical rod structure (or system)".

When implementing the unfolding of a double spherical rod structure in weightlessness, two key technological problems arise – the choice of techniques to activate its motion and selecting the mechanism of fixation (locking) of the unfolding process. The first task relates to the choice of driving forces for initiating the unfolding of rod structures. Not less important is the task to fix the angles between links using specialized devices, built into spherical hinges. In this case, it is necessary to obtain data on the magnitude of forces that occur in nodes at the time of fixation. We propose to use, as a means to initiate the unfolding of a structure, the pulse jet engines (the pyropack type), installed at endpoints of links of the rod structure. We also consider a technique to determine the magnitudes of forces at the nodes of a structure by the moment when the unfolding is over.

It is advisable to explore the dynamics of the process of unfolding a structure in the form of a double spherical rod system based on the Lagrange variational principle. There is a question related to the adaptation to weightlessness of the "oscillation" of a double spherical rod system as the base of a geometrical model for unfolding an orbital object. The answer to this question can be found in the works that address the application of the second-kind Lagrange equations for mechanical systems in weightlessness [3–5]. Formally, it is considered that the calculations regarding the transformation of mechanical rod structures in weightlessness over time can be performed using only the concepts of kinetic energies. That is, when constructing the Lagrange equations of second kind, the potential energy of a conservative mechanical system can be considered as "close to zero". Following the initiation of oscillations by pyrotechnic pulses, the magnitude of kinetic energy for a small period of time should remain unchanged. Such conditions may be rejected in the course of further research.

The specified assumptions make it possible to develop a formal (idealized) approach to the geometrical modeling of the unfolding of rod structures – analogues to double spherical pendulums. In addition, in the process of calculation, it is necessary to prevent the chaotic movements of rod structures. To avoid chaos during shape formation of the structure, it is required to choose such parameters at which the endpoint of the second link should move along a cyclic trajectory.

The value of geometrical modeling manifests itself in the computer-generated animated movies, which visualize the mutual displacements of links in double spherical rod structures in the process of unfolding. Employing the developed models would help at the design stage to calculate the layout and operational parameters of the structure in general.

Thus, the relevance of the chosen subject is emphasized by the need to examine and implement a pulsed device as an easy and cheap driver for the process of unfolding a rod struc-

ture of the double spherical pendulum type. That would be economically justified as in the orbit the process of unfolding the structure is planned to be executed only once. We propose using as such a driver the pulse pyrotechnic jet engines installed at the endpoints of links in a double spherical rod structure. Pyrotechnic devices are much lighter and cheaper compared with known means to initiate the unfolding of a structure. For example, in comparison with electric motors or spring-loaded devices with thermal memory. All this points to the expedience of studying the geometric models of unfolding the rod structures under conditions of weightlessness with pulsed reactive engines at the endpoints of links.

2. Literature review and problem statement

To calculate a geometrical shape of successive phases of unfolding a "pendular" rod structures in the plane, it is advisable to apply studies into dynamics of multi-link pendulums. In practical terms, this represents [6] the construction and solving the Lagrange equations of second kind for the motion of a mechanical system relative to the generalized coordinates. As well as studying the dynamics of a multi-link pendulum, using, for example, the methods of fractional calculus [7]. However, the cited (and similar) papers did not pay enough attention to the graphical interpretation of the obtained solutions.

Frame rope systems are mainly used for the unfolding of rod structures. Papers [8–10] give mathematical models for the process of unfolding a multi-link frame structure with a rope synchronization system. However, the application of a rope unfolding system in practice is limited by the size of a structure and the necessity to synchronize the action of electric motors, which is a separate task given the large number of links. A frame rope system can be considered a prototype of the technique for unfolding a multi-link rod structure considered in this paper.

To analyze numerically the process of unfolding the structures that are transformed, the possibilities of modern software packages that model the dynamics of mechanical systems are utilized. Paper [11] describes a method for the calculation of large-sized structures that can unfold using the program complexes MSC.Software. Paper [12] gives the example of calculating the unfolding applying the package of computer aided dynamic analysis of multicomponent mechanical systems EULER. However, the specified software are not capable, without appropriate add-ins, of implementing the "pulse" techniques for the unfolding of multi-link structures. Other variants of the unfolding systems are described in a review of the scientific literature [13], though there is no information on the "pulse" techniques for unfolding the multi-link rod structures with preference given to the rope systems whose shortcomings were indicated above.

Of theoretical importance for modeling the unfolding of spatial double rod structures are the studies that address the oscillations of spherical and double spherical pendulums. Paper [14] simulated the motion of a spherical pendulum mounted on a rotational platform. Study [15] analyses the dynamics of oscillations of a spherical pendulum with a three-dimensional periodic vibration of the suspension point. The issue of dynamics of a spherical pendulum with a vibratory suspension point was considered in paper [16]. Study [17] investigated, applying the numerical integration of the motion equation, the dynamic turning mode of a flexible

pendulum link in order to increase the smoothness of the drive effort.

Many studies that investigate spatial pendulums are based on the research into spherical pendulum and its variants. Paper [18] examines new models of pendulums, which are considered solid bodies with three rotating degrees of freedom. In such cases it is convenient to employ a single model of a solid body cylinder [19]. Study [20] considered the 3D-pendulum as a solid body, which is held at a fixed hinge with three rotating degrees of freedom. The patterns in spatial mathematical pendulums were considered in papers [21, 22]. However, the results of the specified studies are rather theoretical because it is difficult to apply them as a base for the oscillation simulation algorithm. More complex spatial pendulum configurations are explored as objects of nonlinear analysis, as well as for testing or development of methods to control and stabilize various objects. For example, paper [23] considers a general model of the inverted multiple control over pendulum using a single torque. A similar issue relates to the problem on a pendulum with a movable cart [24]. Paper [25] investigated the inverted double solid-body pendulum, which is controlled by four external momenta. Another broad field of application of pendulum models concerns the damping and stabilization of phenomena, which can be interpreted using a mathematical double-pendulum model [26]. Study [27] reported results of numerical calculations of the complex mechanical system, similar to a double spherical pendulum. It is interesting that the results there are explained using multiple graphical interpretation. Paper [28] examines the model mapping and the visualization of orbits of a double spherical pendulum. In work [29], oscillation parameters of the double spherical pendulum are calculated based on the Lagrangian mechanics. In study [30], double pendulum configurations of the dynamic system are also modeled applying the Lagrangian mechanics, employing the mathematical software packages MapleTM and Matlab. The [31] internet website shows the codes, written in the language of Matlab, for the simulation of oscillations of a double spherical pendulum. However, the cited papers did not provide the graphical confirmation of simulation results.

Studies [32–35] initiated the geometric model of unfolding, in the imaginary plane in weightlessness, a rod structure as the multi-link pendulum. It was believed that the unfolding is driven by the pulsed pyrotechnic jet engines, mounted at the end points of links. The conducted test calculations showed the possibility of using the multi-link rod structures with a common point of attachment. The [36] internet website hosts computer animated images to illustrate the key provisions of a given work.

The results of the scientific literature review [8–30] revealed those issues that have not yet been studied by other authors; that made it possible to state the following task of research. As far as the implementation of the idea of unfolding the spherical two-link structures in weightlessness by the pulses of jet engines, still unresolved are the issues related to the combination of the pulse magnitudes with the generalized coordinates of double spherical rod structures. As well as with the scheme for initiating the motion of a structure elements by the influence of jet pulses on the endpoints of links. Not addressed yet is the task on estimating the magnitude of force, which occurs in the nodal elements at the time

of fixation (locking) of elements of a two-link structure in the unfolded state, calculated in advance.

3. The aim and objectives of the study

The aim of this work is to demonstrate, using specific examples, the geometric model of unfolding, under conditions of weightlessness, a rod structure, similar to a double spherical pendulum. We suggest using the pulse pyrotechnic jet engines mounted at the end points of the structure links to initiate the motion of the structure.

To accomplish the aim, the following tasks have been set:

- to construct and solve a system of the Lagrange differential equations of the second kind to describe in weightlessness the motion of elements of double spherical rod structures;
- in order to simulate the action of pulse jet engines, to develop a scheme of the initiation of motion of double spherical rod structures by the influence of pulses from engines at the endpoints of links;
- using computer animation, to predict over time the mutual arrangement in space of links of double spherical rod structures and to determine, based on it, the time of fixation (locking) of the unfolding, required for the experiment;
- to prevent chaotic motions in the process of unfolding, to design a technique for determining the parameters and initial conditions for the initiation of oscillations of a double rod structure in order to obtain a cyclic trajectory of the endpoint of the second link;
- to construct charts of the time-dependent changes of functions of generalized coordinates, as well as the first and second derivatives of these functions; based on this, to estimate the force characteristics of the system at the time of fixation (locking) of the unfolding;
- to provide test examples of the unfolding of double spherical rod structures in weightlessness.

4. Development of a geometric model of the unfolding process of a rod structure, similar to a double spherical pendulum, in weightlessness

4.1. Explanation of the principle of the unfolding of a rod structure, similar to the spherical and double spherical pendulums

When implementing any scheme of unfolding a rod structure in weightlessness, there is a problem on the choice of driving forces as a means to activate this process. That is, selecting the technical devices or technological processes for initiating the unfolding of rod structures in orbit. In practice, a one-time unfolding is most likely, when a rod structure acquires a geometrical shape and gets fixed immediately after having been delivered to the orbit. In this case, electric motors or other technical devices would become an extra cargo following the unfolding and fixation of the structure. An alternative to this circumstance could be the pyrotechnic pulse jet engines.

To explain the idea of the emergence of motion, we shall consider a non-stretchable rod of length r with point of attachment O , the endpoint of which is the place to where a load with mass m is attached (Fig. 1). Stationarity of the point of attachment is ensured by its attachment to space-

craft whose mass is orders of magnitude larger than the mass of a pendulum cargo.

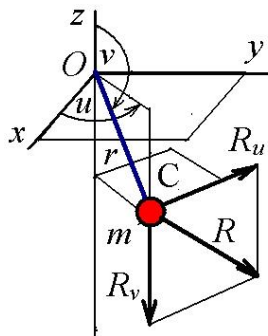


Fig. 1. Schematic of spherical pendulum

The initiation of oscillations in weightlessness of a spherical rod (the name is by analogy with spherical pendulum) is carried out by selecting the direction of action and the magnitude of the pulse applied to the endpoint of the rod using a jet engine of the pulse type. We shall consider the generalized coordinates the angles $u(t)$ and $v(t)$, formed by the horizontal projection of the rod with the Ox axis and the rod with the Oz axis. Denote as virtual vector \mathbf{R}_V the pulse action in the direction of opening the angle v and as virtual vector \mathbf{R}_U – the pulse action in the direction of opening the angle u . The desired direction of pulse action from a jet engine will be defined by the total real vector $\mathbf{R}=\mathbf{R}_U+\mathbf{R}_V$. Location of a jet engine will be related to point C and we shall accept the cargo of the rod structure with mass m .

Initial position of the rod will be defined based on the coordinates of vector $\mathbf{U}_0=\{u(0), v(0)\}$. Expression $\mathbf{U}'_0=\{u'(0), v'(0)\}$ will denote the magnitudes of velocities of oscillation initiation. This expression means that the cargo of mass m is given a pulse of magnitude $mu'(0)$ in the direction of opening the angle u , and at the same time the pulse of magnitude $mv'(0)$ in the direction of opening the angle v . In other words, the opening angles $u(0)$ and $v(0)$ are given initial velocities $u'(0)$ and $v'(0)$, respectively. Given this, a pendulum system must unfold by inertia, which explains the term "inertial unfolding system". As a pyrotechnic pulse jet engine, one can use any device capable of ensuring the magnitude of the pulse, calculated in advance (for example, a pyropack). Therefore, the possibility of applying the estimated magnitudes of pulses from jet engines is based on the relation with the numeric values of instantaneous velocities $u'(0)$ and $v'(0)$.

The calculation of oscillation of a spherical rod structure is performed using the Lagrangian [18], whose notation coincides with the expression for kinetic energy

$$L=0,5rm(x'^2+y'^2+z'^2), \tag{1}$$

where

$$x(t)=r\cos(u(t))\sin(v(t));$$

$$y(t)=r\sin(u(t))\sin(v(t));$$

$$z(t)=r\cos(v(t)). \tag{2}$$

With respect to (2), the expression for the Lagrangian takes the form

$$L=0,5mr^2(u'^2-u'^2\cos^2v+v'^2). \tag{3}$$

Here $u'=\frac{d}{dt}u(t)$; $v'=\frac{d}{dt}v(t)$ are the derivatives from the function of description of the generalized coordinates. Applying expression (3), we obtain a system of two Lagrange equations of the second kind :

$$u''-u''\cos^2v+u'v'\sin 2v=0;$$

$$v''-u'^2\cos v\sin v=0. \tag{4}$$

When solving the system of equations (4), in addition to the length of rod r the cargo mass m , one should take into consideration the values for the initial angle of deviations $\mathbf{U}_0=\{u(0), v(0)\}$, as well as the values of velocities given to the angles of deviations: $\mathbf{U}'_0=\{u'(0), v'(0)\}$. By satisfying the initial conditions, a system of equations (4) is solved approximately using the Runge-Kutta method in the environment of the mathematical software package maple. The derived solutions are conventionally denoted by symbols $U(t), V(t)$. That makes it possible, in the spatial coordinate system $Oxyz$, using formulae (2), to determine coordinates of the link's endpoint (x_C, y_C, z_C) at time point t . To compute these coordinates, in the expressions for functions (2) in the description of coordinates, it is formally needed to replace the lowercase letters u and v with big letters U and V . The approximated shape of the trajectory of displacement of endpoint C will be obtained after we connect the close points by sections

Here are examples that show the results of motion of a spherical rod in weightlessness (Fig. 2, a). To compare the displacement trajectories of an endpoint of the rod, we shall also show the results of oscillation in the field of Earth gravity (Fig. 2, b) under the same initial conditions. Motion parameters are as follows: $r=1$; $m=1$; $\mathbf{U}_0=\{0, \pi/2\}$, $\mathbf{U}'_0=\{1.56, 2\}$. Integration time $T=5$.

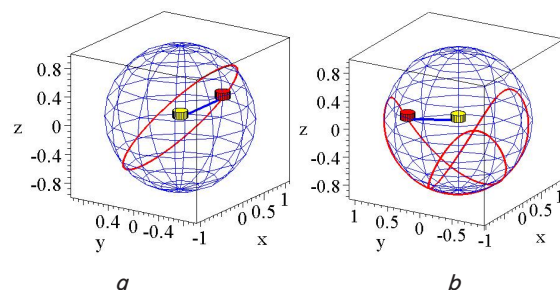


Fig. 2. Motion trajectory of point C: a – in weightlessness; b – in the field of Earth gravity

Next, consider the motion of a double spherical rod structure in weightlessness. It is believed that the double rod structure is attached to a spherical hinge, fixed on a space craft. Mass of the space craft is orders of magnitude larger than the total mass of elements of the structure, which is why the attachment node is considered stationary. We shall also accept that rods are made of lightweight and strong carbon fiber, so the entire mass of the rod structure will be concentrated in the cargos of nodular points. A beginning of the first link is attached to a fixed point O, and the beginning of the second link is attached to the end point of the first link with coordinates (x_1, y_1, z_1) (Fig. 3). The generalized coordinates are considered to be angles $u_1(t)$ and $v_1(t)$, as well $u_2(t)$

and $v_2(t)$, formed by the appropriate horizontal projections of rods with the Ox axis, as well as the respective rods with the Oz axis (Fig. 3).

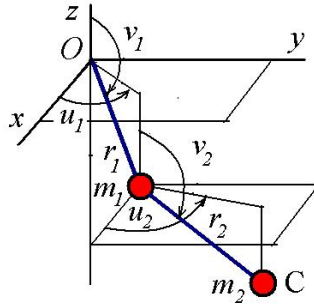


Fig. 3. Schematic of double spherical rod structure

The initiation of oscillations of a double spherical rod structure in weightlessness is performed similarly to the spherical rod from the previous example. Specifically, by choosing the direction of action and the magnitude of pulses given to the endpoints of a pendulum links using jet engines of the pulse type. Virtual vector \mathbf{R}_{V1} is the result of the pulse action in the direction of opening the angle v_1 ; and virtual vector \mathbf{R}_{U1} is obtained as a result of the pulse action in the direction of opening the angle u_1 . The summary real vector $\mathbf{R}_1 = \mathbf{R}_{U1} + \mathbf{R}_{V1}$ defines the required direction of the pulse action of the first jet engine. Similarly, virtual vector \mathbf{R}_{V2} is the result of the pulse action in the direction of opening the angle v_2 ; and virtual vector \mathbf{R}_{U2} is derived as the result of the pulse action in the direction of opening the angle u_2 . The summary real vector $\mathbf{R}_2 = \mathbf{R}_{U2} + \mathbf{R}_{V2}$ defines the required direction of the pulse action of the second jet engine.

The initial position of the double rod structure will be determined based on the coordinates of vector $\mathbf{U}_0 = \{u_1(0), v_1(0), u_2(0), v_2(0)\}$. Expression $\mathbf{U}'_0 = \{u'_1(0), v'_1(0), u'_2(0), v'_2(0)\}$ will denote the magnitudes of velocities of oscillation initiation. This expression means that the cargo with mass m_1 was given the pulse of magnitude $m_1 u'_1(0)$ in the direction of opening the angle u_1 , and at the same time the pulse of magnitude $m_1 v'_1(0)$ in the direction of opening the angle v_1 . The same applies to the second pair of angles and mass m_2 . Hence it follows that the opening angles $u_1(0)$ and $v_1(0)$ are given initial velocities $u'_1(0)$ and $v'_1(0)$, and the opening angles $u_2(0)$ and $v_2(0)$ – velocities $u'_2(0)$ and $v'_2(0)$, respectively. Therefore, the possibility of using the estimated magnitudes of the pulses from jet engines is also based on the relation with the numerical values of instantaneous velocities $u'(0)$ and $v'(0)$.

The requirements to manage the action of pyrotechnic engines of the rod structure imply specific conditions for the design of a spherical hinge, located between the links of the structure. Namely, a spherical hinge in the node should provide for the unfolding of its links under condition of the existence of two axes of rotation, which run through the center point of the hinge. This can be achieved through the proper design of a spherical hinge in the pendulum node, which was described, for example, in papers [37, 38].

The important issues related to the organization of motion of a rod structure include the possibility to prevent chaotic movements of rod structures. This is achieved through a proper selection of magnitudes of pyrotechnic engines to ensure

the movements of elements that are comprehensible during calculations. This can be achieved by organizing the cyclic non-chaotic trajectories of the endpoint of the second link.

4. 2. Determining a non-chaotic cyclic trajectory of the motion of an endpoint of the second link of a rod spherical structure

To understand the nature of oscillations of two-link spherical rod structures, one must have the predicted motion trajectory of an endpoint of the second link of the pendulum. An acceptable curve in this case would be a non-chaotic cyclic trajectory. A cyclic trajectory is believed to be the displacement trajectory of endpoint $C(x_C, y_C, z_C)$ of the two-link structure whose geometrical shape is periodically repeated (possibly, approximately). The cyclic character of a trajectory is ensured by a proper choice of parameters for a two-link spherical structure and by the initial conditions of its motion.

Condition $\mathbf{U}_0 = \{u_1(0), v_1(0), u_2(0), v_2(0)\}$ satisfies the "starting" geometrical shape of the structure. In our case, it should take a "folded" form, suitable to deliver into orbit. For example, the following examples will employ condition $\mathbf{U}_0 = \{0, \pi/2, -\pi, \pi/2\}$. To adjust the shape of the trajectory, there remains the condition $\mathbf{U}'_0 = \{u'_1(0), v'_1(0), u'_2(0), v'_2(0)\}$, which defines the magnitudes of velocities of oscillation initiation. The magnitudes of pyrotechnic charges should be aligned with these velocities.

Thus, the question arises: how can we find, for the values of the initial deviation angles $\mathbf{U}_0 = \{u_1(0), v_1(0), u_2(0), v_2(0)\}$, for the lengths of links $\mathbf{L} = \{r_1, r_2\}$, and the values of cargo masses $\mathbf{m} = \{m_1, m_2\}$, such values for the velocities of deviations $\mathbf{U}'_0 = \{u'_1(0), v'_1(0), u'_2(0), v'_2(0)\}$ so that the trajectory of the endpoint of the second link would have a cyclical nature?

Paper [39] described a technique to define a set of parameters of pendulum oscillations (in the field of Earth gravity, which does not compromise generalization), which could ensure the cyclic displacement trajectory of the second cargo, for example, a double pendulum. We shall give an interpretation of the technique at the level of graphical explanations. The main idea is the following. Let there be a conservative oscillatory system whose description includes, among others, a generalized coordinate – denote it as function $u(t)$. We shall numerically solve the Lagrangian differential equations of the second kind and build an approximated image of the integral curve in phase space $\{u, Du, t\}$ of the generalized variable $u(t)$. The image will consist of a set of line segments that connect successive points, obtained as a result of an approximate solution to the equation. This visualization will depend on a certain value of the "controlling" parameter of the problem, or the value of the initial condition (denote it as p). The random values of p will result in the formation in phase space $\{u, Du, t\}$ of a "chaotic" integral curve whose projection onto the phase plane $\{u, Du\}$ would be also a "chaotic" phase trajectory (Fig. 4, a). Selecting a random value for p during calculation will lead to the chaotic oscillations of the pendulum cargo.

In the case of changing the values for the "controlling" parameter p , the character of the phase trajectory must change appropriately. At the critical value $p = p_0$, the character of the phase trajectory will change at the qualitative level; it will turn into a "focused" curve (Fig. 4, b). In the phase plane $\{u, Du\}$, one would observe a kind of the optical effect, "sharpening" the chaos of phase trajectories (paper [39] called this phenomenon a projection focusing).

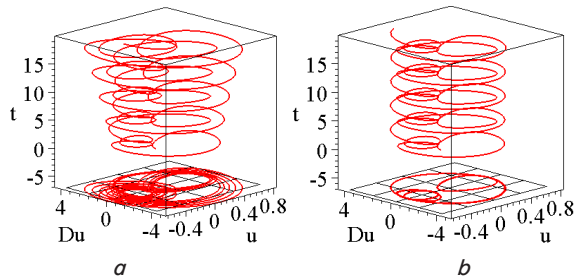


Fig. 4. Integral curves and phase trajectories for: *a* – random value of *p*; *b* – computed value $p=p_0$

Taking into consideration the value of parameter $p=p_0$ in the process of solving a Lagrange equation of the second kind make it possible to calculate the coordinates of points, which should sit along the non-chaotic trajectory of the pendulum trace. So, the non-chaotic technological oscillation trajectories of an element of the pendulum mechanical system are shown in the images of phase trajectories in the form of "focused" curves. This can be formulated as follows: the critical value of parameter *p* will be obtained at the time when the image of the projection of the integral curve onto a phase plane (that is, the phase trajectory) acquires the minimum area (in pixel dimension).

In practice, the reported approach was implemented using the graphical information processing library Imaobtainools from the maple software package. Below is the corresponding text from a fragment of the program.

Assume we have *S* arrays of points under condition that the *s*-th among them defines a family of curves, $\mathbf{x}[i] := \text{solu}(\mathbf{w}); \mathbf{y}[i] := \text{dsolu}(\mathbf{w})$, when parameters *s* and *w* change in a single step from zero to *S* and *W*, respectively. To form the image and to analyze it, we shall use the software maple, fragments of which are shown in Fig. 5, *a-c*.

```

for s from 0 to S do:
Gr[s] := pointplot({seq([x[i],
y[i]], i = 0..W)}, axes = NONE,
color = black, symbol = point);
end do:

a

for i from 0 to S do
plotsetup(bitmap, plotoutput =
cat('C://TEMP//', i, '. ', bitmap));
display(Gr[i]);
plotsetup(default)
end do:

b

for i from 0 to S do
img[i] := Read(cat(cat(cat
("C://TEMP/", i), ".bmp")))
end do:
for s from 0 to S do:
R := 1:G := 1:B := 1:kk := 0:
for i to N do for j to M do
if `and`(`and`(img[s][i,j,1] =
R, img[s][i, j, 2] = G),
img[s][i, j, 3] = B)
then kk := kk+1 end if
end do end do:
K[s] := N*M - kk;
end do:
min([seq(K[s], s=0..S)]).

c
    
```

Fig. 5. Blocks of the program to form the image and to analyze it: *a* – forming a bitmap image of the curve; *b* – converting a bitmap image of the curve into a graphic file; *c* – determining the value *s*, which corresponds to the minimum number of pixels in the image

The result of execution of the program is the determined value of parameter *s*, which would match the minimum number of pixels in a rectangle of pixels of size *N* per *M*. By using the found parameter *s*, one could calculate the value of the controlling parameter and to map the non-chaotic cyclic trajectory of the second cargo of the pendulum. The values of all parameters are given in conventional values.

4. 3. Geometric modeling of oscillations of a double spherical pendulum in weightlessness

We shall calculate the oscillations of a double spherical rod structure using the Lagrangian [28] whose notation coincides with the expression for kinetic energy

$$L = 0,5r_1m_1(x_1'^2 + y_1'^2 + z_1'^2) + 0,5r_2m_2(x_2'^2 + y_2'^2 + z_2'^2), \tag{5}$$

where

$$\begin{aligned} x_1(t) &= r_1 \cos(u_1(t)) \sin(v_1(t)); \\ y_1(t) &= r_1 \sin(u_1(t)) \sin(v_1(t)); \\ z_1(t) &= r_1 \cos(v_1(t)); \\ x_c(t) &= r_1 \cos(u_1(t)) \sin(v_1(t)) + r_2 \cos(u_2(t)) \sin(v_2(t)); \\ y_c(t) &= r_1 \sin(u_1(t)) \sin(v_1(t)) + r_2 \sin(u_2(t)) \sin(v_2(t)); \\ z_c(t) &= r_1 \cos(v_1(t)) + r_2 \cos(v_2(t)). \end{aligned} \tag{6}$$

Using the Lagrangian (5) and formulae (6), we build a system of four Lagrange equations of the second kind:

$$\begin{aligned} \frac{d}{dt} \left(\frac{\partial L}{\partial u_1'} \right) - \frac{\partial L}{\partial u_1} &= 0; \quad \frac{d}{dt} \left(\frac{\partial L}{\partial v_1'} \right) - \frac{\partial L}{\partial v_1} = 0; \\ \frac{d}{dt} \left(\frac{\partial L}{\partial u_2'} \right) - \frac{\partial L}{\partial u_2} &= 0; \quad \frac{d}{dt} \left(\frac{\partial L}{\partial v_2'} \right) - \frac{\partial L}{\partial v_2} = 0. \end{aligned} \tag{7}$$

Here

$$\begin{aligned} u_1' &= \frac{d}{dt} u_1(t); \quad v_1' = \frac{d}{dt} v_1(t); \\ u_2' &= \frac{d}{dt} u_2(t); \quad v_2' = \frac{d}{dt} v_2(t) \end{aligned}$$

are the derivatives from the function of description of the generalized coordinates. Equations (7) in the expanded form are not given due to their cumbersome form. We employed the mathematical software package maple, able to operate with information in the form of analytical expressions. For example, to operate with the derived "computer" approximated solution to a differential equation as a normal function.

When solving the system of Lagrange equations of the second kind, one should consider coordinates of such vectors as: the lengths of links: $\mathbf{L}=\{r_1, r_2\}$; the values of cargo masses: $\mathbf{m}=\{m_1, m_2\}$; the values for the initial deviation angles: $\mathbf{U}_0=\{u_1(0), v_1(0), u_2(0), v_2(0)\}$, as well as the values for velocities given to the deviation angles: $\mathbf{U}_0'=\{u_1'(0), v_1'(0), u_2'(0), v_2'(0)\}$.

By satisfying the initial conditions, the system of the Lagrange equations of the second kind (7) was solved approximately, using the Runge-Kutta method, in the environment of the mathematical software package maple. The solutions obtained are conditionally indicated by symbols $U_1(t)$, $V_1(t)$, $U_2(t)$, $V_2(t)$. This allows us to determine, in the spatial $Oxyz$ coordinate system, using formulae (6), the "real" coordinates of the endpoint nodal point (x_C, y_C, z_C) of the second link of the pendulum at time t . To compute these coordinates, one must formally replace, in the expressions of functions (6) that describe coordinates of the nodal elements of pendulum, the lowercase letters u and v with big letters U and V [34]. The approximated form of the displacement trajectory of endpoint point C will be obtained after we connect close points by segments.

Below are the examples of geometric modeling of the unfolding of two-link spherical rod mechanisms. Values of all parameters are given in conventional values. Given that a two-link structure is delivered into orbit in the folded form, in all the examples one of the initial conditions will take the form of $\mathbf{U}_0 = \{0, \pi/2, -\pi, \pi/2\}$. We also consider $m_1=1$ and $m_2=1$. Force characteristics are calculated as the product of masses by the value of the second derivative (acceleration). In the examples given below we calculated systems composed of six double spherical rod structures within the plane with a common fixed point [32]. Angles between the starting locations of rod structures are $\pi/3$ (Fig. 6).

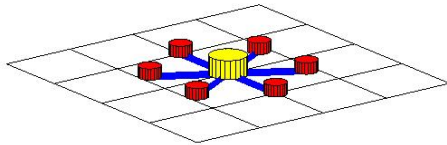


Fig. 6. Starting position of six two-link structures within plane

We have calculated and constructed for each example:

- the values of velocities given to the deviation angles, which ensure a cyclic non-chaotic trajectory of the endpoint of the second rod structure and its image;
- certain phases in the location of links of two-link rod mechanisms in the process of unfolding;
- phase trajectories of functions of the generalized coordinates that correspond to a cyclic non-chaotic trajectory of the endpoint of the second link;
- time-dependent charts of change in the values of angles as functions of the generalized coordinates, as well as the first (velocity) and second (acceleration) derivatives from these functions;
- based on the acceleration charts, we mapped the diagrams of force characteristics that arise in the moment of locking the unfolding of structures:

$$Fu_1 = m_1 d^2 u_1(t) dt^2; Fv_1 = m_1 d^2 v_1(t) dt^2;$$

$$Fu_2 = m_2 d^2 u_2(t) dt^2; Fv_2 = m_2 d^2 v_2(t) dt^2;$$

- variants of the unfolding of six two-link rod mechanisms with a common fixed point.

The [36] internet site hosts the animated images of the unfolding processes of double spherical rod structures.

Example 1. $r_1=2; r_2=1; \mathbf{U}_0 = \{1, -1.024, 1.9, 0.5\}$. Integration time $T=6.6$. Fig. 7 shows a cyclic trajectory of endpoint C and a position of the double structure at some point of time. Fig. 8 shows phase trajectories of functions of the gen-

eralized coordinates that correspond to a cyclic non-chaotic trajectory of the endpoint of the second link.

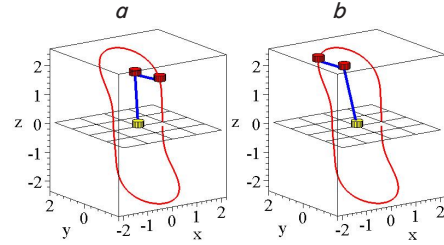


Fig. 7. Cyclic motion trajectory of point C for example 1: $a - t=0.858; b - t=1.98$

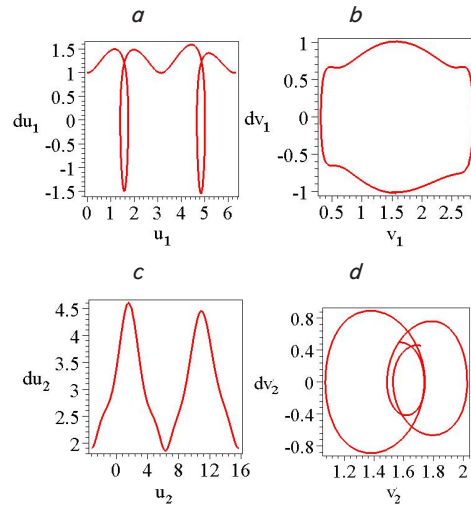


Fig. 8. Phase trajectories of generalized coordinates for example 1: $a - u_1(t); b - v_1(t); c - u_2(t); d - v_2(t)$

Fig. 9–12 show time-dependent charts of change in the magnitudes of angles as functions of the generalized coordinates, the first derivatives from these functions, as well as the diagrams of force characteristics arising at the time of locking the unfolding of a structure.

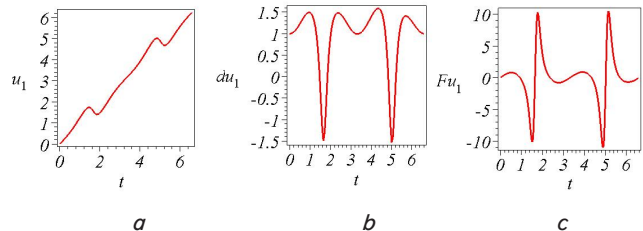


Fig. 9. Charts of generalized coordinate $u_1(t)$ of the first link: $a - u_1(t); b - du_1(t)/dt; c - Fu_1$

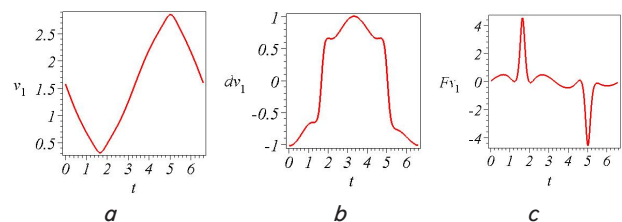


Fig. 10. Charts of generalized coordinate $v_1(t)$ of the first link: $a - v_1(t); b - dv_1(t)/dt; c - Fv_1$

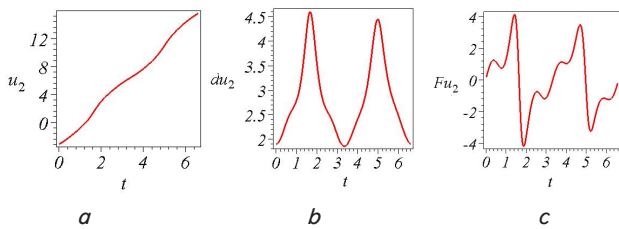


Fig. 11. Charts of generalized coordinate $u_2(t)$ of the second link: $a - u_2(t)$; $b - du_2(t)/dt$; $c - Fu_2$

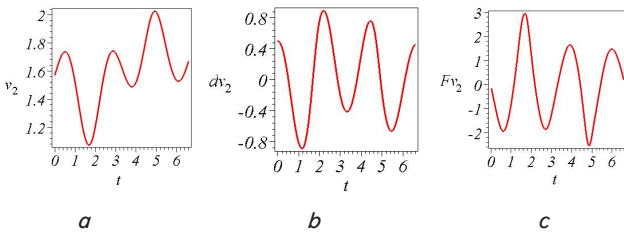


Fig. 12. Charts of generalized coordinate $v_2(t)$ of the second link: $a - v_2(t)$; $b - dv_2(t)/dt$; $c - Fv_2$

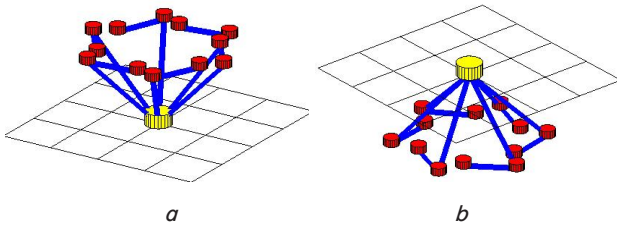


Fig. 13. Certain spatial structures depending on the time of unfolding: $a - t=2.4$; $b - t=4.1$

Example 2. $r_1=1$; $r_2=2$; $U_0'=\{3, 3, -0.5, 0.5\}$. Integration time $T=2.95$. Fig. 14 shows a cyclic motion trajectory of endpoint C, as well as the position of a double structure over certain moments of time; Fig. 15 shows phase trajectories of functions of the generalized coordinates.

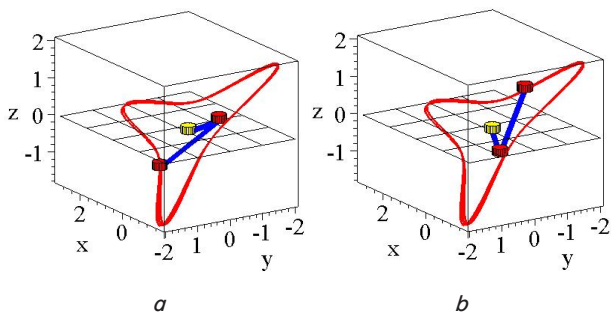


Fig. 14. Cyclic motion trajectory of point C for example 2: $a - t=0.9$; $b - t=2.44$

Fig. 16–19 show the time-dependent charts of changes in the magnitudes of angles as functions of the generalized coordinates, the first derivatives from these functions, as well as the diagrams of force characteristics arising at the time of locking the unfolding of a structure.

Fig. 20 shows the time-dependent variants of the unfolding of six two-link rod mechanisms with a common fixed point for example 2.

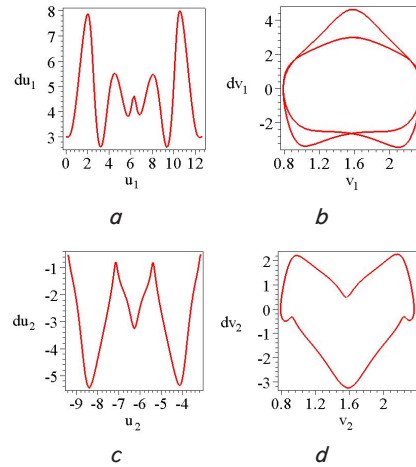


Fig. 15. Phase trajectories of generalized coordinates for example 2: $a - u_1(t)$; $b - v_1(t)$; $c - u_2(t)$; $d - v_2(t)$

Example 3. We show the formation of multi-link structures similar to the geometrical models of sections of foldable trusses [1, 2]. We accept $r_1=1$; $r_2=2$; $U_0'=\{1, -4.9, -1, 3\}$. Integration time $T=6.2$. Fig. 21 shows a cyclic motion trajectory of endpoint C, as well as the position of a double structure over certain moment of time; Fig. 22 shows phase trajectories of functions of the generalized coordinates.

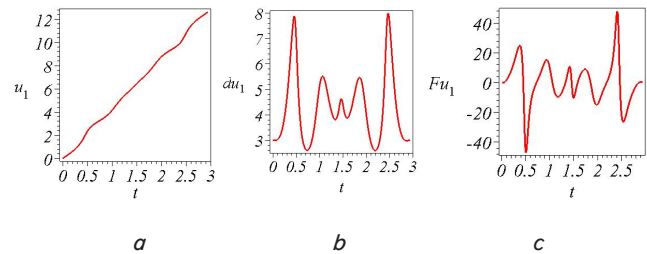


Fig. 16. Charts of generalized coordinate $u_1(t)$ of the first link: $a - u_1(t)$; $b - du_1(t)/dt$; $c - Fu_1$

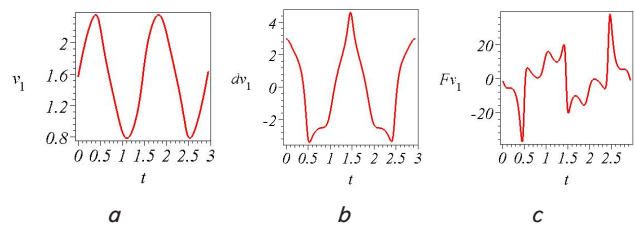


Fig. 17. Charts of generalized coordinate $v_1(t)$ of the first link: $a - v_1(t)$; $b - dv_1(t)/dt$; $c - Fv_1$

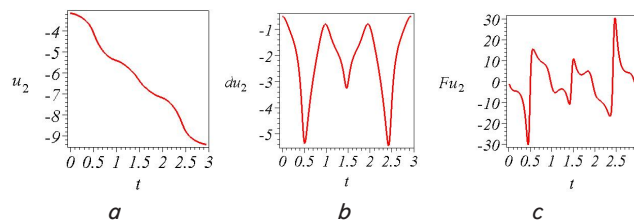


Fig. 18. Charts of generalized coordinate $u_2(t)$ of the first link: $a - u_2(t)$; $b - du_2(t)/dt$; $c - Fu_2$

Fig. 23–26 show the time-dependent charts of changes in the magnitudes of angles as functions of the generalized co-

ordinates, the first derivatives from these functions, as well as the diagrams of force characteristics arising at the time of locking the unfolding of a structure.

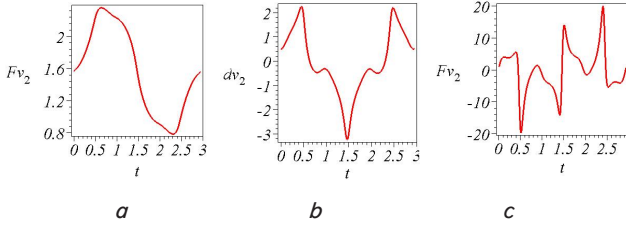


Fig. 19. Charts of generalized coordinate $v_1(t)$ of the first link: $a - v_2(t)$; $b - dv_2(t)/dt$; $c - Fv_2$

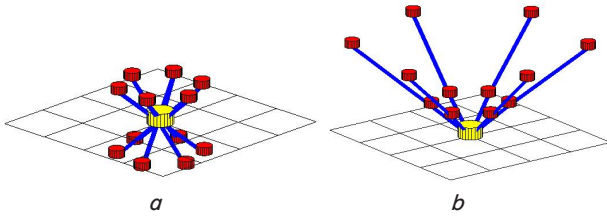


Fig. 20. Certain spatial structures dependent on time: $a - t=2$; $b - t=2.45$

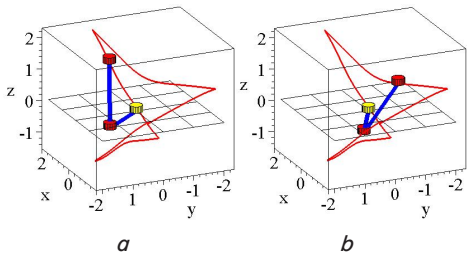


Fig. 21. Cyclic motion trajectory of point C for example 2: $a - t=3.5$; $b - t=4.8$

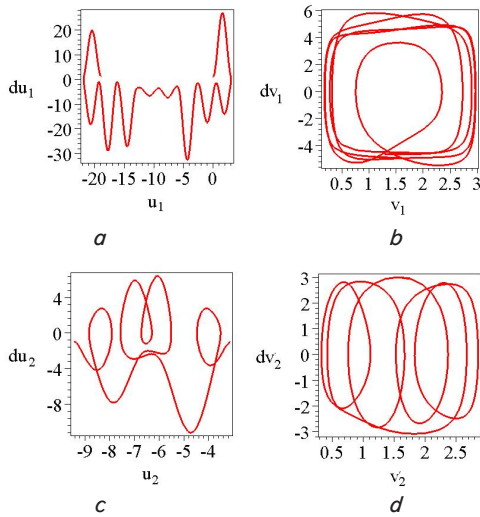


Fig. 22. Phase trajectories of the generalized coordinates for example 2: $a - u_1(t)$; $b - v_1(t)$; $c - u_2(t)$; $d - v_2(t)$

Fig. 23–26 show the time-dependent charts of changes in the magnitudes of angles as functions of the generalized coordinates, the first derivatives from these functions, as well as the diagrams of force characteristics arising at the time of locking the unfolding of a structure.

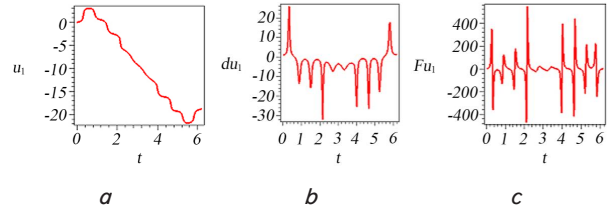


Fig. 23. Charts of generalized coordinate $u_1(t)$ of the first link: $a - u_1(t)$; $b - du_1(t)/dt$; $c - Fu_1$

Fig. 27 shows the time-dependent variants of the unfolding of six two-link rod mechanisms with a common fixed point for example 3. The obtained structures' shape is similar to the models of sections of foldable trusses [1, 2].

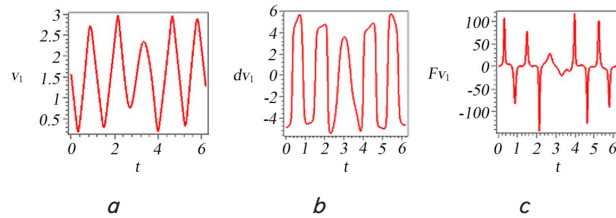


Fig. 24. Charts of generalized coordinate $v_1(t)$ of the first link: $a - v_1(t)$; $b - dv_1(t)/dt$; $c - Fv_1$

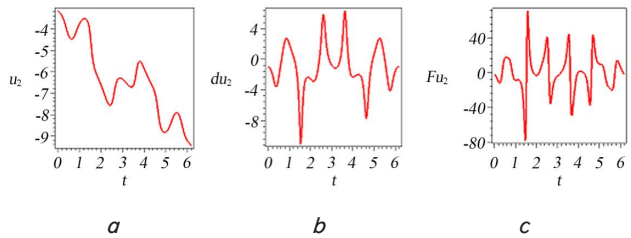


Fig. 25. Charts of generalized coordinate $u_1(t)$ of the first link: $a - u_2(t)$; $b - du_2(t)/dt$; $c - Fu_2$

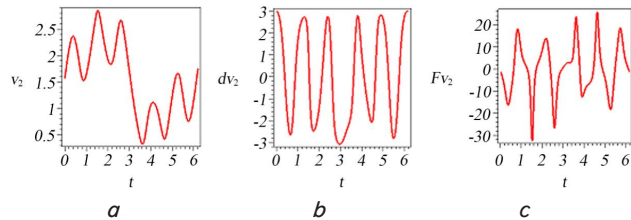


Fig. 26. Charts of generalized coordinate $v_1(t)$ of the first link: $a - v_2(t)$; $b - dv_2(t)/dt$; $c - Fv_2$

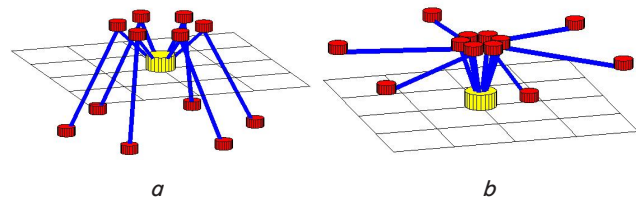


Fig. 27. Certain spatial structures dependent on the time of unfolding: $a - t=2.6$; $b - t=5.2$

In the figures that show the charts of functions of the generalized coordinates, we pay attention to the diagrams of force characteristics arising at the time of locking the unfold-

ing of a structure. To this end, one should analyze values of charts of functions

$$Fu_1=m_1d^2u_1(t)dt^2; Fv_1=m_1d^2v_1(t)dt^2;$$

$$Fu_2=m_2d^2u_2(t)dt^2; Fv_2=m_2d^2v_2(t)dt^2$$

at the endpoint of the interval of integration $t=6.2$. After computing, the following values are obtained

$$Fu_1(6.2)=2.63; Fv_1(6.2)=-1.54;$$

$$Fu_2(6.2)=0.63; Fv_2(6.2)=-1.24.$$

The value of these functions at the endpoint of the interval of integration will define the force, which will act on the nodal element of a rod structure at the moment of locking its unfolding. The reliability of these results can be checked after watching computer animated images at the [36] internet site.

5. Discussion of results on the simulation of unfolding in the weightlessness of rod structures similar to two-link spherical pendulums

Our paper reports the obtained idealized geometric models of the unfolding of rod structures similar to double spherical pendulums. As the engines for the process of unfolding, we propose the pulse pyrotechnic jet engines installed at endpoints of links in the rod structure. Pyrotechnic engines are much lighter and cheaper compared to other motors. Such engines could be used when the unfolding of a structure in orbit should be carried out only once, as is often the case. Delivery of pyrotechnic engines from Earth into orbit would be economically expedient in comparison with electric motors or spring devices with thermal memory.

The advantages of the considered inertial technique of unfolding in the weightlessness of the rod structure similar to a double spherical pendulum include the following:

- the technology of the inertial technique for unfolding the rod structures is not fundamentally critical to the size of links in the structure;
- based on the scheme for unfolding a single rod structure, it is possible to form many-ray schemes with many spherical structures with a fixed attachment node;
- there is no need to create and synchronize the means of control over the magnitudes of angles at separate nodes of a multi-link structure.

The results obtained can be explained by the possibility of applying the variational principle of Lagrange to the calculation of mechanical structures with respect to the above-specified features. That allowed us to use the Lagrange equations of the second kind to describe the motion of an analog of a double spherical pendulum in weightlessness, regardless of the location of links in a rod structure.

We are aware of the fact that the geometric model of a double spherical rod structure in weightlessness requires further research to bring it closer to an actual structure. It is necessary to take into consideration the moments of inertia of rods at the rotation of the structure's elements. The development of this direction of research implies the use of other

variants of double spherical rod structures. Detailed studies are also needed into design of a spherical hinge.

The difficulties in the development of research in a given direction might arise when solving the inverse problem of assembly. That is, given the preset resultant location of a pendulum's elements, it would be necessary to define a rational set of parameters for a double spherical rod structure and initial conditions of its movement, which will enable such an unfolding. Additional complexity relates to taking into consideration the fact that the inverse problem has several solutions.

7. Conclusions

1. The obtained solutions to the Lagrangian systems of differential equations of the second kind allowed us to approximately describe the motion in weightlessness of a rod structure similar to a double spherical pendulum. That made it possible to implement specific geometric models of the unfolding of two-link spherical rod structures and to observe them under the mode of computer animation.

2. To simulate the action of a pulse pyrotechnic jet engine, we developed a scheme for initiating the motion of a two-link spherical rod structure by the impact from pulses to the endpoints of its links.

The pulse of action on a link of the rod structure will be numerically proportional to the value of the first derivative from the function that describes a change in the magnitude of the respective angle as a generalized coordinate. That allowed us to demonstrate geometric models of action from the pulse jet engines as the drivers to the process of unfolding two-link rod structures.

3. Using computer animation, we predicted the time-dependent position of links in double spherical rod structures, obtained as a result of the inertial unfolding of links applying the pulse jet engines. That makes it possible to determine the current values of angles between the links. An analysis of successive animation frames enables determining the moment of fixation (locking) of the unfolding when the links of double spherical rod structures would acquire the required spatial position.

4. We propose a technique for determining the parameters and initial conditions for the initiation of oscillations of a double rod structure in order to obtain a non-chaotic cyclic trajectory of the endpoint of the second link. For example, choosing initial velocities $U_0'=\{1, -4.9, -1, 3\}$ at $r_1=1$ i $r_2=2$ makes it possible to prevent the chaotic movements of links in a double spherical rod structure in the process of unfolding.

5. Our studies resulted in the construction of the time-dependent charts of change in the functions of the generalized coordinates, as well as the first and second derivatives from these functions; based on this, it was possible to estimate the force characteristics of the system at the time of fixation (locking) the unfolding. The obtained phase trajectories of the unfolding process allow us to estimate the speed of the structures' elements at the point of breaking the unfolding.

6. Quantitative characteristics of the given coordinate-wise graphical construction confirm the computer-animated images of unfolding in weightlessness of certain variants of double spherical rod structures.

References

1. A new family of deployable mechanisms based on the Hoekens linkage / Lu S., Zlatanov D., Ding X., Molfino R. // *Mechanism and Machine Theory*. 2014. Vol. 73. P. 130–153. doi: <https://doi.org/10.1016/j.mechmachtheory.2013.10.007>
2. Tibert G. Deployable tensegrity structures for space applications. Stockholm, 2002. 242 p.
3. Szuminski W. Dynamics of multiple pendula. University of Zielona Gora, Olsztyn, 2012. 57 p.
4. Szuminski W. Dynamics of multiple pendula. University of Zielona Gora, Olsztyn, 2013. 32 p.
5. Szuminski W. Dynamics of multiple pendula without gravity // Conference: Conference: Chaos 2013, Volume: Chaotic Modeling and Simulation (CMSIM). 2014. Issue 1. P. 57–67. URL: https://www.researchgate.net/publication/285143816_dynamics_of_multiple_pendula_without_gravity
6. Martinez-Alfaro H. Obtaining the dynamic equations, their simulation, and animation for N pendulums using Maple. URL: <http://www2.esm.vt.edu/~anayfeh/conf10/Abstracts/martinez-alfaro.pdf>
7. Lopes A. M., Tenreiro Machado J. A. Dynamics of the N-link pendulum: a fractional perspective // *International Journal of Control*. 2016. Vol. 90, Issue 6. P. 1192–1200. doi: <https://doi.org/10.1080/00207179.2015.1126677>
8. Kinematic analysis of the deployable truss structures for space applications / Yan X., Fu-ling G., Yao Z., Mengliang Z. // *Journal of Aerospace Technology and Management*. 2012. Vol. 4, Issue 4. P. 453–462. doi: <https://doi.org/10.5028/jatm.2012.04044112>
9. Deployable Perimeter Truss with Blade Reel Deployment Mechanism. NASA's Jet Propulsion Laboratory, Pasadena, California, 2016. URL: <https://www.techbriefs.com/component/content/article/tb/techbriefs/mechanics-and-machinery/24098>
10. Bushuyev A., Farafonov B. Mathematical modeling of the process of disclosure of a large-scale solar battery // *Mathematical Modeling and Numerical Methods*. 2014. Issue 2. P. 101–114.
11. Schesnyak S., Romanov A. Designing and calculating large-scale unfolding structures using software packages MSC.Software // *CADmaster*. 2009. Issue 2-3. P. 28–36.
12. Boykov V. Program complex of automated dynamic analysis of EULER multicomponent mechanical systems // *CAD and graphics*. 2009. Issue 9. P. 17–20.
13. Features of the Calculation Deployment Large Transformable Structures of Different Configurations / Zimin V., Krylov A., Meshkovskii V., Sdobnikov A., Fayzullin F., Churilin S. // *Science and Education of the Bauman MSTU*. 2014. Issue 10. P. 179–191. doi: <https://doi.org/10.7463/1014.0728802>
14. Zel'dovich B. Y., Soileau M. J. Bi-frequency pendulum on a rotary platform: modeling various optical phenomena // *Uspekhi Fizicheskikh Nauk*. 2004. Vol. 174, Issue 12. P. 1337–1354. doi: <https://doi.org/10.3367/ufnr.0174.200412e.1337>
15. Petrov A. Asymptotic integration of Hamiltonian systems // *Mechanics of the solid*. 2005. Issue 35. P. 84–91.
16. Glukhikh Y. Oscillations of a spherical pendulum with a vibrating suspension point // *Mechanics of a rigid body*. 2005. Issue 35. P. 109–114.
17. Loveykin V., Rybalko V., Melnichenko V. Investigation of the fluctuations of cargo on a flexible suspension under the operation of the mechanism of rotation of the jib crane // *Scientific Bulletin of the National University of Bioresources and Natural Resources of Ukraine*. 2011. Issue 166. P. 115–121.
18. Dynamics and control of a 3D pendulum / Shen J., Sanyal A. K., Chaturvedi N. A., Bernstein D., McClamroch H. // 2004 43rd IEEE Conference on Decision and Control (CDC) (IEEE Cat. No.04CH37601). 2004. doi: <https://doi.org/10.1109/cdc.2004.1428650>
19. Chaturvedi N. A., McClamroch N. H. Asymptotic stabilization of the hanging equilibrium manifold of the 3D pendulum // *International Journal of Robust and Nonlinear Control*. 2007. Vol. 17, Issue 16. P. 1435–1454. doi: <https://doi.org/10.1002/rnc.1178>
20. Nonlinear Dynamics of the 3D Pendulum / Chaturvedi N. A., Lee T., Leok M., McClamroch N. H. // *Journal of Nonlinear Science*. 2010. Vol. 21, Issue 1. P. 3–32. doi: <https://doi.org/10.1007/s00332-010-9078-6>
21. Náprstek J., Fischer C. Types and stability of quasi-periodic response of a spherical pendulum // *Computers & Structures*. 2013. Vol. 124. P. 74–87. doi: <https://doi.org/10.1016/j.compstruc.2012.11.003>
22. Consolini L., Tosques M. On the exact tracking of the spherical inverted pendulum via an homotopy method // *Systems & Control Letters*. 2009. Vol. 58, Issue 1. P. 1–6. doi: <https://doi.org/10.1016/j.sysconle.2008.06.010>
23. Anan'evskii I. M., Anokhin N. V. Control of the spatial motion of a multilink inverted pendulum using a torque applied to the first link // *Journal of Applied Mathematics and Mechanics*. 2014. Vol. 78, Issue 6. P. 543–550. doi: <https://doi.org/10.1016/j.jappmath-mech.2015.04.001>
24. Lee T., Leok M., McClamroch N. H. Dynamics and control of a chain pendulum on a cart // 2012 IEEE 51st IEEE Conference on Decision and Control (CDC). 2012. doi: <https://doi.org/10.1109/cdc.2012.6427059>
25. Xinjilefu, Hayward V., Michalska H. Hybrid Stabilizing Control for the Spatial Double Inverted Pendulum // *Advances in Intelligent and Soft Computing*. 2010. P. 201–215. doi: https://doi.org/10.1007/978-3-642-16259-6_16
26. Egger P., Caracoglia L. Analytical and experimental investigation on a multiple-mass-element pendulum impact damper for vibration mitigation // *Journal of Sound and Vibration*. 2015. Vol. 353. P. 38–57. doi: <https://doi.org/10.1016/j.jsv.2015.05.003>

27. Ludwicki M., Kudra G., Awrejcewicz J. Axially excited spatial double pendulum nonlinear dynamics. URL: https://www.researchgate.net/profile/Jan_Awrejcewicz/publication/288669893_Axially_excited_spatial_double_pendulum_nonlinear_dynamics/links/568b788908ae051f9afb07e4/Axially-excited-spatial-double-pendulum-nonlinear-dynamics.pdf
28. Marsden J., Scheurle J., Wendlandt J. Visualization of Orbits and Pattern Evocation for the Double Spherical Pendulum. URL: [https://authors.library.caltech.edu/20096/1/MaScWe1996\(2\).pdf](https://authors.library.caltech.edu/20096/1/MaScWe1996(2).pdf)
29. Marsden J. E., Scheurle J. Lagrangian reduction and the double spherical pendulum // ZAMP Zeitschrift für angewandte Mathematik und Physik. 1993. Vol. 44, Issue 1. P. 17–43. doi: <https://doi.org/10.1007/bf00914351>
30. Dehlin F., Askolsson J. Modelling and Simulation of Conservative Dynamical Systems by Computer Algebra Assisted Lagrangian Mechanics. Sweden, 2017. 80 p.
31. Double spherical pendulum. URL: <https://www.mathworks.com/matlabcentral/fileexchange/37363-double-spherical-pendulum>
32. Geometrical modeling of the inertial unfolding of a multi-link pendulum in weightlessness / Kutsenko L., Shoman O., Semkiv O., Zapolsky L., Adashevskay I., Danylenko V. et. al. // Eastern-European Journal of Enterprise Technologies. 2017. Vol. 6, Issue 7 (90). P. 42–50. doi: <https://doi.org/10.15587/1729-4061.2017.114269>
33. Kutsenko L. M. Illustrations to Geometric Modeling of Inertial Disclosure of Multilayer Rod Construction in Weightlessness. URL: <http://repositsc.nuczu.edu.ua/handle/123456789/4868>
34. Geometrical modeling of the shape of a multilink rod structure in weightlessness under the influence of pulses on the end points of its links / Kutsenko L., Semkiv O., Zapolskiy L., Shoman O., Ismailova N., Vasyliiev S. et. al. // Eastern-European Journal of Enterprise Technologies. 2018. Vol. 2, Issue 7 (92). P. 44–58. doi: <https://doi.org/10.15587/1729-4061.2018.126693>
35. Kutsenko L. M. Illustrations to geometric modeling of oscillations of multi-faceted bar constructions in the absence of weight under the influence of pulses on the final points of the links. URL: <http://repositsc.nuczu.edu.ua/handle/123456789/6335>
36. Kutsenko L. M. Illustrations to the geometric modeling of the opening of the weightlessness of a rod construction in the form of a double spherical pendulum under the influence of pulses on the end points of its links. URL: <http://repositsc.nuczu.edu.ua/handle/123456789/6864>
37. Navarro Heredia A. L. Spatial Operator Algebra in Modeling and Properties of 3D Inverted Pendulae. McGill University Montreal, Canada, 2017. 121 p.
38. Ludwicki M., Awrejcewicz J., Kudra G. Spatial double physical pendulum with axial excitation: computer simulation and experimental set-up // International Journal of Dynamics and Control. 2014. Vol. 3, Issue 1. P. 1–8. doi: <https://doi.org/10.1007/s40435-014-0073-x>
39. Development of projection technique for determining the non-chaotic oscillation trajectories in the conservative pendulum systems / Semkiv O., Shoman O., Sukharkova E., Zhurilo A., Fedchenko H. // Eastern-European Journal of Enterprise Technologies. 2017. Vol. 2, Issue 4 (86). P. 48–57. doi: <https://doi.org/10.15587/1729-4061.2017.95764>